

See discussions, stats, and author profiles for this publication at: <https://www.researchgate.net/publication/51865872>

Anti-leishmanial activity of the bisnaphthalimidopropyl derivatives

ARTICLE in PARASITOLOGY INTERNATIONAL · DECEMBER 2011

Impact Factor: 1.86 · DOI: 10.1016/j.parint.2011.11.005 · Source: PubMed

CITATIONS

3

READS

22

6 AUTHORS, INCLUDING:



Ali Ouaisi

French National Centre for Scientific Resea...

164 PUBLICATIONS **3,860** CITATIONS

SEE PROFILE



Ana Marta Silva

University of Porto

10 PUBLICATIONS **100** CITATIONS

SEE PROFILE



Nilanjan Roy

ARIBAS

89 PUBLICATIONS **1,015** CITATIONS

SEE PROFILE



Anabela Cordeiro-da-Silva

University of Porto

103 PUBLICATIONS **1,768** CITATIONS

SEE PROFILE

Bisnaphthalimidopropyl Derivatives as Inhibitors of *Leishmania* SIR2 Related Protein 1

Joana Tavares,^[a] Ali Ouaisi,^[a, b] Paul Kong Thoo Lin,^[c] Inês Loureiro,^[a] Simranjeet Kaur,^[d] Nilanjan Roy,^[d] and Anabela Cordeiro-da-Silva^{*[a]}

The NAD⁺-dependent deacetylases, namely sirtuins, are involved in the regulation of a variety of biological processes such as gene silencing, DNA repair, longevity, metabolism, apoptosis, and development. An enzyme from the parasite *Leishmania infantum* that belongs to this family, LiSIR2RP1, is a NAD⁺-dependent tubulin deacetylase and an ADP-ribosyltransferase. This enzyme's involvement in *L. infantum* virulence and survival underscores its potential as a drug target. Our search for selective inhibitors of LiSIR2RP1 has led, for the first time, to the identification of the antiparasitic and anticancer bisnaphthalimidopropyl (BNIP) alkyl di- and triamines (IC₅₀ values

in the single-digit micromolar range for the most potent compounds). Structure–activity studies were conducted with 12 BNIP derivatives that differ in the length of the central alkyl chain, which links the two naphthalimidopropyl moieties. The most active and selective compound is the BNIP diammononane (BNIPDanon), with IC₅₀ values of 5.7 and 97.4 μM against the parasite and human forms (SIRT1) of the enzyme, respectively. Furthermore, this compound is an NAD⁺-competitive inhibitor that interacts differently with the parasite and human enzymes, as determined by docking analysis, which might explain its selectivity toward the parasitic enzyme.

Introduction

Proteins that belong to the silent information regulator 2 (SIR2) family, also known as sirtuins, are present in a variety of organisms from bacteria to humans.^[1] They are involved in the regulation of a number of biological processes such as heterochromatin formation, gene silencing, DNA repair, development, longevity, metabolism, adipogenesis, and apoptosis (reviewed in reference [2]). Indeed, these proteins are classified as class III histone deacetylases, owing to their dependence on NAD⁺ to deacetylate lysine residues of histones and non-histone substrates.^[3–5] Apart from the deacetylase activity, some sirtuins also exhibit ADP-ribosyltransferase activity.^[6,7]

Recent findings suggest a direct link between the activity of sirtuins and diseases such as cancer, HIV, and Parkinson's disease.^[8–12] The first reports on sirtuin inhibitors identified, apart from the physiological inhibitor nicotinamide, synthetic inhibitors such as sirtinol and splitomicin (Figure 1).^[13,14] Because these three compounds exhibit weak inhibitory properties, subsequent structure–activity studies led to the identification of more potent derivatives such as HR73 and β-phenylsplitomicin.^[8,15,16] Furthermore, high-throughput screening against the human sirtuin SIRT1 led to the identification of an indole derivative (see Figure 1) as the most potent (IC₅₀ < 0.1 μM) and selective inhibitor over two other NAD⁺-dependent deacetylases, SIRT2 and SIRT3, described so far.^[17] In addition, drugs that mimic adenosine (suramin) or that target enzymes or receptors, such as kinases, that bind to adenosine-containing cofactors or ligands have been identified as human SIR2 inhibitors.^[18,19] Moreover, the recently reported co-crystal structure of a SIRT5–suramin complex has shed more light on the molecular nature of SIRT5 enzyme inhibition.^[20]

Leishmaniasis is a parasitic disease caused by the protozoan parasites of the genus *Leishmania*, and is characterized by diverse clinical manifestations varying from localized ulcerative skin lesions to disseminated visceral infection. The latter is fatal when left untreated. *Leishmania* infects vertebrate hosts via the bite of a sand fly (*Phlebotomus* and *Lutzomyia* spp.) during a blood meal, through the inoculation of infective flagellated promastigotes that invade or are phagocytosed by local or recruited host cells. In the phagolysosomes, the promastigotes differentiate into non-flagellated amastigotes, which multiply

[a] Dr. J. Tavares, Dr. A. Ouaisi, I. Loureiro, Prof. Dr. A. Cordeiro-da-Silva
IBMC – Instituto de Biologia Molecular e Celular
Universidade do Porto
Rua do Campo Alegre 823, 4150-180 Porto (Portugal)
and
Laboratório de Bioquímica
Faculdade de Farmácia da Universidade do Porto
R. Aníbal Cunha no. 164, 4050-047 Porto (Portugal)
Fax: (+351) 226 099 157
E-mail: cordeiro@ibmc.up.pt

[b] Dr. A. Ouaisi
INSERM, CNRS, UMR 5235, Université de Montpellier 2
Bâtiment 24-CC 107, Pl. Eugène Bataillon
34095 Montpellier Cedex 5 (France)

[c] Prof. Dr. P. Kong Thoo Lin
The Robert Gordon University
School of Pharmacy and Life Sciences
St. Andrew Street, Aberdeen AB25 1HG, Scotland (UK)

[d] S. Kaur, Dr. N. Roy
Centre of Pharmacoinformatics
National Institute of Pharmaceutical Education and Research
Sector 67, SAS Nagar 160062, Punjab (India)

Supporting information for this article is available on the WWW under <http://dx.doi.org/10.1002/cmdc.200900367>.

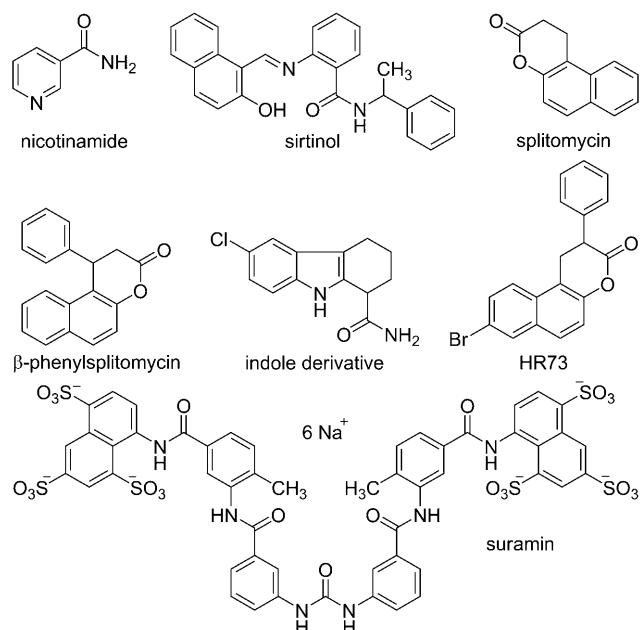


Figure 1. Examples of NAD⁺-dependent SIR2 inhibitors.

and are able to infect other adjacent or distant macrophages. The classical treatment is currently unsatisfactory owing to side effects, the emergence of resistance, and the need for increased efficacy in immunosuppressed patients, especially due to HIV co-infection. During the past few years we have been interested in the protozoan parasite *Leishmania infantum* SIR2-related protein 1 (LiSIR2RP1) due to its role in the survival and virulence of the parasite.^[21,22] Indeed, this cytosolic parasite protein, partially associated with the microtubule network, is a NAD⁺-dependent tubulin deacetylase and an ADP-ribosyltransferase.^[23]

In previous studies we have shown that bisnaphthalimidopropyl (BNIP) polyamine derivatives exert anti-leishmanial activity in vitro, inducing the death of promastigote forms by apoptosis.^[24] The search for target-specific SIR2 inhibitors led us to evaluate whether BNIP derivatives can selectively inhibit the parasitic enzyme.^[24–26]

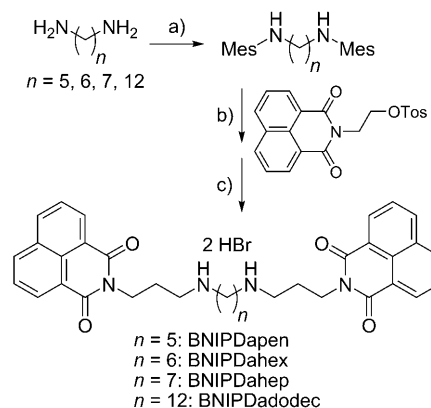
Herein we report the first structure–activity relationship study of 12 BNIP derivatives with regard to their activity against human SIRT1 (hSIRT1) and the parasitic enzyme, LiSIR2RP1. The compounds differed in the length of the central alkyl chains, with 2, 3, or 4 nitrogen atoms, linking the two naphthalimidopropyl groups. We found that the most potent and selective inhibitor of LiSIR2RP1 is the BNIP diammononane **6**, which has an alkyl linker containing nine methylene groups and two NH groups. Furthermore, this compound is an NAD⁺-competitive inhibitor, and results from our molecular docking analysis suggest how it interferes differently with LiSIR2RP1 than with hSIRT1; this could explain the greater selectivity of compound **6** toward the parasitic enzyme.

Results and Discussion

Chemistry

We previously reported the synthesis of compounds such as (bisnaphthalimidopropyl)putrescine (BNIPPut), -spermidine (BNIPSpd), -spermine (BNIPSpm), and the bisnaphthalimidopropyl di- and triamines such as BNIPDaoct, BNIPDanon, BNIPDadec, BNIPDeta, and BNIPDpta.^[25–27] The same methodology was used to carry out the synthesis of new compounds BNIPDapen (**2**), BNIPDahex (**3**), BNIPDahep (**4**), and BNIPDadodec (**8**).

The synthesis essentially involves a three-step reaction. Penta-, hexa-, hepta- and dodeca-diamines were first mesitylated with mesityl chloride in pyridine at room temperature. N-alkylation between the *N*-mesityl alkyl diamines and *o*-tosylpropyl naphthalimide^[26] gave the corresponding protected compounds, which upon treatment with hydrobromic acid/glacial acetic acid yielded their respective products in high yields (80–94%; Scheme 1)



Scheme 1. Reagents and conditions: a) MesCl/pyridine, room temperature; b) DMF/Cs₂CO₃, 85 °C, 12 h; c) HBr/glacial acetic acid, CH₂Cl₂, room temperature, 12 h.

Enzyme inhibition

All BNIP derivatives and some of the commercially available sirtuin inhibitors such as nicotinamide, sirtinol, and suramin were tested in vitro for their ability to inhibit the *L. infantum* (LiSIR2RP1) and human (hSIRT1) forms of sirtuin. Experiments were conducted with a commercially available fluorimetric deacetylase assay. This coupled enzymatic assay uses a dual fluorophore- and quencher-labeled peptide that contains an acetylated lysine as substrate. After the peptide is deacetylated by sirtuin activity, it becomes a substrate for proteolysis by lysyl endopeptidase, resulting in separation of the quencher from the fluorophore; the ensuing fluorescence is then measured (see scheme S1, Supporting Information). To determine if the apparent inhibitory activity observed for the compounds tested is not due to inhibition of the intermediate proteolysis step, we measured the effect of each compound on this lysyl endopeptidase with a deacetylated peptide in place of the

acetylated one. None of the compounds was able to inhibit lysyl endopeptidase, confirming that inhibition is due to their interference with the NAD^+ -dependent deacetylase activity of LiSIR2RP1 or hSIRT1 (see figure S1, Supporting Information).

We recently demonstrated that LiSIR2RP1 is an ADP-ribosyl-transferase and an NAD^+ -dependent deacetylase that can be inhibited in a noncompetitive manner by nicotinamide.^[23] The mechanism by which nicotinamide inhibits the deacetylase activity of sirtuins is already known. In fact, nicotinamide inhibits these enzymes by interfering with an intermediate reaction. The positively charged *O*-alkyl amidate intermediate and nicotinamide are generated after the nucleophilic attack of the acetyl lysine carbonyl oxygen on the C1' to the nicotinamide ribose of NAD^+ .^[6,28,29] When nicotinamide binds to the enzyme containing the *O*-alkyl amidate intermediate, both can react in a process known as nicotinamide exchange, in which the NAD^+ and the acetylated peptide are reformed.^[6,28,30] In the presence of high concentrations of nicotinamide, this reaction occurs at the expense of deacetylation. The results listed in Table 1 indicate that LiSIR2RP1 is more sensitive to nicotinamide inhibition ($\text{IC}_{50} = 39.4 \pm 5.0 \mu\text{M}$) than hSIRT1 ($\text{IC}_{50} = 118.3 \pm 23.6 \mu\text{M}$). This could be due to differences in the flexible loop

Table 1. Inhibition of *L. infantum* SIR2RP1 (LiSIR2RP1) and human SIRT1 (hSIRT1) by known sirtuin inhibitors.

Compound	$\text{IC}_{50} [\mu\text{M}]^{[a]}$		SI ^[b]
	LiSIR2RP1	hSIRT1	
nicotinamide	39.4 ± 5.0	118.3 ± 23.6	3.00
sirtinol	193.8 ± 31.8	245.5 ± 3.5	1.28
suramin	6.8 ± 0.7	2.4 ± 0.5	0.35

[a] Concentration of drug required to inhibit 50% of enzymatic activity relative to control; data are reported as the mean \pm SD of at least three independent experiments. [b] Selectivity index = $(\text{IC}_{50} \text{ hSIRT1})/(\text{IC}_{50} \text{ LiSIR2RP1})$.

of the respective enzymes, which seems to be involved in the recognition of different substrates, and its close contact with the C pocket. Indeed, Avalos and colleagues^[31] disclosed the mechanism of sirtuin inhibition by nicotinamide, highlighting the role of the C pocket. A structure-based mechanism was proposed, in which nicotinamide can be present in either a reactive or an entrapped conformation, and the *O*-alkyl amidate intermediate can exist in a contracted or extended conformation; these seem to be key factors for deacetylation or the nicotinamide exchange reaction. Furthermore, varying sensitivities to nicotinamide inhibition were reported for the yeast SIR2 in complexes with different proteins.^[32]

Sirtinol has low inhibitory potency toward the *L. infantum* enzyme, with an IC_{50} value of $193.8 \pm 31.8 \mu\text{M}$ (Table 1). The IC_{50} value toward hSIRT1 determined in this study ($245.5 \pm 3.5 \mu\text{M}$, Table 1) is higher than that reported by others.^[15] This could be due to its low aqueous solubility, although no significant difference in sirtinol's potency toward the parasite and human sirtuin forms was observed.

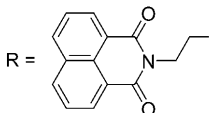
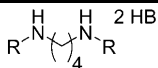
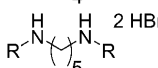
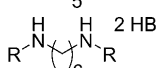
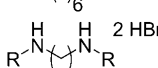
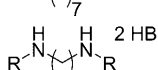
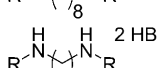
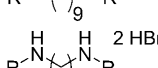
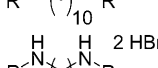
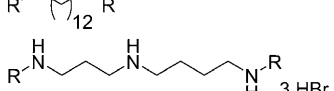
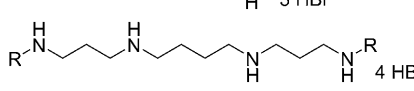
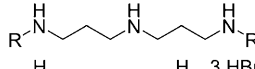
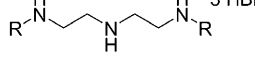
Suramin is a symmetric polyanionic naphthylurea originally used to treat sleeping sickness and onchocerciasis. Several other biological functions have been attributed to this compound and its derivatives, such as antiproliferative and antiviral activities.^[33] Although suramin has been shown to interfere with numerous proteins, we thought it would be interesting to investigate whether it can act as an inhibitor of LiSIR2RP1 versus hSIRT1. Indeed, we show herein that suramin is a more active inhibitor of hSIRT1 ($\text{IC}_{50} = 2.4 \pm 0.5 \mu\text{M}$) than of LiSIR2RP1 ($\text{IC}_{50} = 6.8 \pm 0.7 \mu\text{M}$; Table 1). The inhibitory activity toward hSIRT1 agrees with the results reported by Schuetz and colleagues.^[20] Furthermore, the structural basis of hSIRT5 inhibition by suramin reveals that this molecule interacts with the B and C pockets of the NAD^+ binding site as well as with the substrate binding site. Additionally, suramin acts as a linker molecule, leading to the dimerization of hSIRT5.^[20] A similar mechanism of inhibition has been suggested by molecular docking and analysis of favorable interactions with human SIRT1 and SIRT2.^[19]

A series of bisnaphthalimidopropyl diamine derivatives containing an alkyl linker with 4 (compound 1) to 11 (compound 8) methylene units were synthesized. We reasoned that with increasing length of the alkyl chain, the two naphthalimido rings are less likely to undergo π - π stacking interactions. The effect of introducing positive charges, through nitrogen atoms, on the bisnaphthalimido linker was also evaluated with compounds 9–12. All of the tested bisnaphthalimidopropyl derivatives are capable of inhibiting the NAD^+ -dependent deacetylase activity of LiSIR2RP1, with IC_{50} values $< 55 \mu\text{M}$. The most active compound against this enzyme, compound 6, exhibited an IC_{50} value in the single-digit micromolar range ($5.7 \pm 0.2 \mu\text{M}$; Table 2). On the other hand, the least effective compound was 12, with an IC_{50} value of $54.7 \pm 15.7 \mu\text{M}$ (Table 2). The selectivity index, which is the ratio of the inhibitory potencies of the BNIP derivatives toward LiSIR2RP1 versus hSIRT1, appears to depend on the length and net charge of the linker group. Indeed, BNIP diamine derivatives containing 4–7 methylene units (compounds 1–4) in the linker are less active than those containing 8–12 methylene units (compounds 5–8). The optimal distance between the two naphthalimidopropylamine groups that results in the most potent inhibitory activity toward LiSIR2RP1 was observed with compound 6, the linker group of which contains nine methylene units. The introduction of positive charges in the linker does not improve potency. For example, compound 9 has eight atom units in the linker, of which seven are carbon and one is a nitrogen atom, and it is less active ($\text{IC}_{50} = 17.9 \pm 1.6 \mu\text{M}$) than compound 5, which contains eight carbons ($\text{IC}_{50} = 9.2 \pm 1.4 \mu\text{M}$; Table 2).

All BNIP derivatives were less potent against hSIRT1 than toward the LiSIR2RP1. The IC_{50} values obtained with hSIRT1 vary between 43.1 and 182.8 μM (Table 2).

In contrast to our observations with LiSIR2RP1, changes in the linker do not significantly affect the potency of these compounds toward hSIRT1. Indeed, the most active compound on this enzyme is 11, with an IC_{50} value of $43.1 \pm 9.3 \mu\text{M}$. These results suggest a certain degree of selectivity in some BNIP derivatives toward the parasite enzyme. The highest selectivity for

Table 2. Inhibition of *L. infantum* SIR2RP1 (LiSIR2RP1) and human SIRT1 (hSIRT1) by BNIP derivatives.

			IC ₅₀ [μM] ^[a]		SI ^[b]
Compound		Structure	LiSIR2RP1	hSIRT1	
1	BNIPDabut		35.0 ± 5.8	73.1 ± 14.9	2.1*
2	BNIPDapen		37.7 ± 6.9	82.2 ± 16.4	2.2*
3	BNIPDahep		43.3 ± 9.5	93.5 ± 7.8	2.2**
4	BNIPDahep		52.7 ± 5.2	127.5 ± 31.9	2.4*
5	BNIPDaoct		9.2 ± 1.4	116.5 ± 23.3	12.7**
6	BNIPDanon		5.7 ± 0.2	97.4 ± 4.9	17.0***
7	BNIPDadec		11.2 ± 1.6	113.8 ± 22.7	10.2**
8	BNIPDadodec		10.1 ± 1.2	94.7 ± 23.7	9.4**
9	BNIPSpd		17.9 ± 1.6	94.8 ± 23.7	5.3**
10	BNIPSpm		39.5 ± 6.5	102.2 ± 31.9	2.6**
11	BNIPDpta		32.8 ± 2.4	43.1 ± 9.3	1.3
12	BNIPDeta		54.7 ± 15.7	182.8 ± 22.2	3.3**

[a] Data are reported as the mean ± SD of at least three independent experiments. [b] Selectivity index = (IC₅₀hSIRT1)/(IC₅₀LiSIR2RP1); **p* < 0.05, ***p* < 0.01, ****p* < 0.001 between LiSIR2RP1 and hSIRT1.

SIR2RP1.^[34] Therefore, this might explain the discrepancies between the IC₅₀ values.

Complementary experiments were done using an alternative method to evaluate the inhibitory effect of the BNIP derivatives on the NAD⁺-dependent deacetylase activity of LiSIR2RP1. In a previous report we showed that, in the presence of NAD⁺, LiSIR2RP1 deacetylates purified tubulin.^[23] The reaction could be inhibited by nicotinamide and visualized by western blot using specific antibodies raised against either total α-tubulin or its acetylated form.^[23] Figure 2 shows the effect of increasing concentrations of nicotinamide or compound 7 (each at 0.125, 0.25 and 0.5 mM) on NAD⁺-dependent deacetylation of tubulin (0.5 μg) mediated by rLiSIR2RP1 (0.5 μg). Because DMSO was used to dissolve compound 7, increasing amounts of DMSO (0.25, 0.5 and 1%) corresponding to the percentage present in each assay were used as controls. As expected, none of the DMSO concentrations inhibited tubulin deacetylation by LiSIR2RP1. In contrast, increasing amounts of compound 7 or nicotinamide were capable of inhibiting tubulin deacetylation mediated by LiSIR2RP1.

LiSIR2RP1 was observed with compound 6, followed by compounds 5 and 7, as they are respectively 17-, 12.7-, and 10.2-fold more active against LiSIR2RP1 than hSIRT1.

In parallel, we examined the potential of BNIP molecules to exert anti-leishmanial activity particularly toward the form of the parasite that is present in the human host. The data show that the molecules indeed exert an efficient anti-intracellular amastigote activity, with IC₅₀ values ranging from 1.01 ± 0.39 to 9.52 ± 0.56 μM (Table 3). It is not surprising that we observed no straight correlation between the inhibitory activities of BNIP compounds toward the enzymatic activity of LiSIR2RP1 and intracellular amastigote proliferation. Indeed, the enzyme assays were conducted with 0.25 μg of recombinant LiSIR2RP1 (rLiSIR2RP1), whereas LiSIR2RP1 is only weakly expressed in wild-type parasites. In fact, in a previous study, in order to co-immunoprecipitate a sufficient quantity of interacting LiSIR2RP1 partner(s) for identification by mass spectrometry, we were compelled to use transfected parasites overexpressing Li-

Table 3. Effect of BNIP derivatives on the intracellular development of *L. infantum* amastigotes.

Compound		IC ₅₀ [μM] ^[a]
1	BNIPDabut	4.53 ± 0.54
2	BNIPDapen	1.26 ± 0.18
3	BNIPDahep	3.46 ± 0.48
4	BNIPDahep	1.12 ± 0.0084
5	BNIPDaoct	2.43 ± 0.19
6	BNIPDanon	6.03 ± 0.67
7	BNIPDadec	1.02 ± 0.41
8	BNIPDadodec	1.01 ± 0.39
11	BNIPDpta	4.22 ± 1.07
12	BNIPDeta	9.52 ± 0.56

[a] PMA-differentiated THP-1 cells infected with amastigotes were incubated with a series of compound concentrations over 3 days. The growth inhibitory effect of the compounds was determined by luciferase assay, and IC₅₀ values were determined by linear regression analysis; each experiment was performed in triplicate, and values represent the mean ± SD obtained for at least three independent experiments.

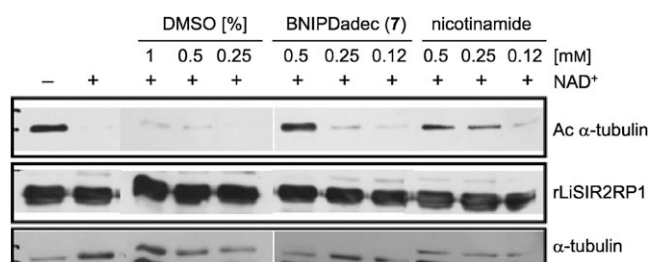


Figure 2. Compound **7** inhibits the deacetylation of α -tubulin by LiSIR2RP1: Purified tubulin dimers were incubated overnight at room temperature with purified rLiSIR2RP1 in the presence or absence of NAD^+ (1 mM) and nicotinamide or compound **7** (each at 0.5, 0.25, 0.125, 0 mM). The percentage of DMSO (1, 0.5, and 0.25%) present in each concentration of compound **7** was also evaluated. The reaction products were analyzed by western blot with specific antibodies to acetylated α -tubulin, α -tubulin, and LiSIR2RP1 as indicated.

To further analyze the inhibitory activity of BNIP derivatives, kinetics studies were performed with rLiSIR2RP1 and its most active inhibitor, **6**, by combining various drug and NAD^+ concentrations (Figure 3). A similar approach was conducted using increasing amounts of acetylated peptide substrate; the results are shown as Lineweaver–Burk plots. Compound **6** did not act as a competitive inhibitor of the LiSIR2RP1 substrate (Figure 3a). Its inhibitory effect on LiSIR2RP1 deacetylase activity is due to competition with NAD^+ (Figure 3b). The K_M values obtained for NAD^+ differed in the presence of compound **6** at 0,

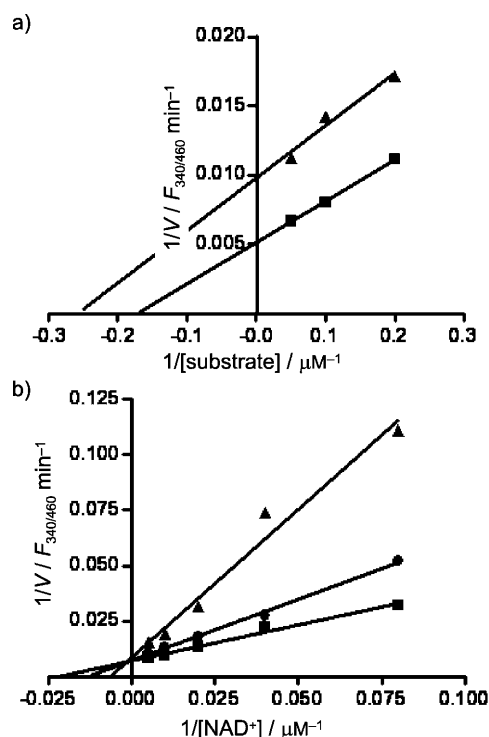


Figure 3. Kinetics of inhibition of LiSIR2RP1 by compound **6**: The rate of substrate deacetylation in the CycLex SIRT1/Sir2 deacetylase fluorimetric kit was measured in the presence (▲, ●) or absence (■) of compound **6** (7.5 μM); the concentration of substrate was fixed at 10 μM . a) Inhibition by compound **6** as a function of substrate concentration; the concentration of NAD^+ was fixed at 200 μM . b) Inhibition by **6** at 6 μM (▲) and at 3 μM (●) as a function of NAD^+ concentration (12.5, 25, 50, 100, and 200 μM).

3, or 6 μM ($K_M = 45.0, 78.14,$ and $149.9 \mu\text{M}$, respectively), while no significant differences were observed between their respective V_{max} values (138.9, 140.8, and $112.4 F_{340/460} \text{ min}^{-1}$). Based on these data, we hypothesize that **6** interacts with the NAD^+ binding site of the enzyme, or at least close enough to induce structural changes that interfere with NAD^+ binding.

Suramin and other related adenosine receptor antagonists, such as kinase inhibitors, were reported to be sirtuin inhibitors.^[18–20,35] In fact, the screen of a library of kinase inhibitors led to the identification of a disubstituted bis(indol)maleimide as a potent and competitive inhibitor of NAD^+ (IC_{50} values of 3.5 and 0.8 μM against hSIRT1 and hSIRT2, respectively).^[18]

Examination of the inhibitor binding site

To determine the potential structural differences between LiSIR2RP1 and hSIRT1, a homology model of both proteins was built and analyzed. The homology model of LiSIR2RP1 showed 40% identity with the template human SIRT2 as reference (PDB code: 1J8F).^[36] The region showing 41% identity with the template (residues 242–525) was modeled out of a total of 747 amino acids in hSIRT1. The evaluation of these models using PROCHECK revealed that 93% of the residues are in the most favored regions of the Ramachandran plot for both models, with 0.4% of the residues in disallowed regions for hSIRT1. No residue was in the disallowed regions of the Ramachandran plot for LiSIR2RP1. The overall quality factor of the models was 78% for hSIRT1 and 66% for LiSIR2RP1. Based on this information, the homology models were considered to be reliable.

Four BNIP derivatives, (compounds **6**, **7**, and **8**, with low IC_{50} values) and compound **3** (with a high IC_{50} value), were selected for docking to validate the inhibitory action of these inhibitors on LiSIR2RP1. It was found that all of these compounds acting at the NAD^+ binding pocket, hence showing competition with NAD^+ (data not shown), which is in agreement with our experimental data. Compound **6** was found to be the best suited as an inhibitor among all other BNIP derivatives, owing to its lowest docking score and higher interaction with the target. Structural comparison of the binding pockets of LiSIR2RP1 and hSIRT1 revealed a highly conserved NAD^+ binding site; however, the binding mode of compound **6** differed considerably between the two proteins (Figure 4). The docking scores of compound **6** on LiSIR2RP1 and hSIRT1 are -17.2 and -15.8 , and the numbers of hydrogen bonds formed are six and five, respectively. In hSIRT1, compound **6** interacts with Arg 274, Ser 442, and Asn 465 in the A pocket, and with Gln 345 in the B pocket; it is directed away from the C pocket, as shown in Figure 4. Compound **6** shows an interaction with the adenine sub-pocket (A pocket) and C pocket (NAD^+ hydrolysis region) in LiSIR2RP1. The residues involved in hydrogen bonding with **6** in LiSIR2RP1 include Ala 40, Gly 216, and Asn 241 present in the A pocket, and Asn 125 in the C pocket. The C pocket comprises residues Ser 43, His 106, Asp 127 and Asn 125, and is reported to be involved in the polarization and hydrolysis of the NAD^+ glycosidic bond, leading to the formation of the enzyme–ADP-ribose intermediate, as cited for human SIRT2.^[37] The interaction of **6** with C pocket residues may interfere with

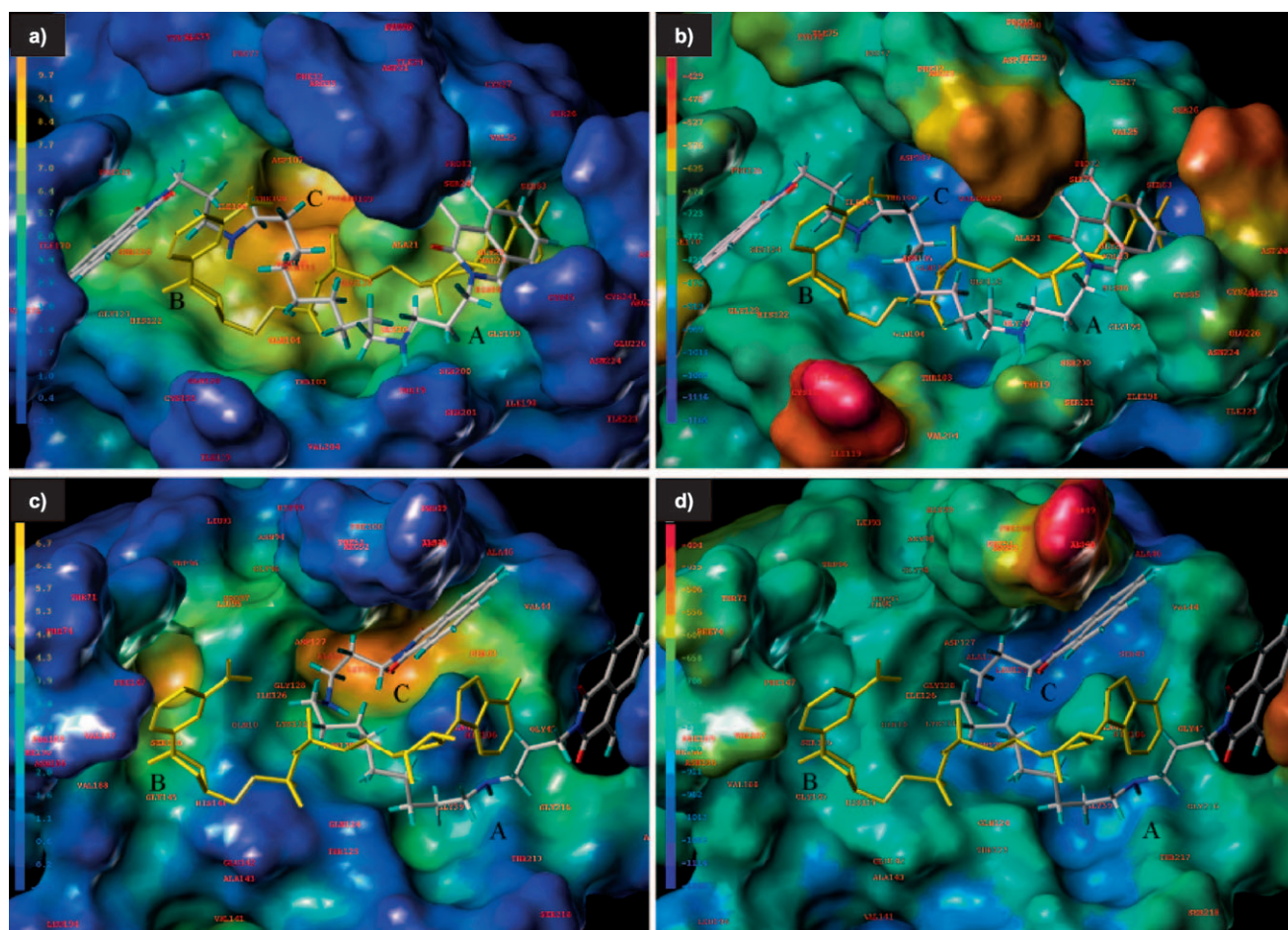


Figure 4. Cavity depth (a,c) and electrostatic surface analysis (b,d) for the binding pockets of: a,b) hSIRT1 and c,d) LiSIR2RP1. The NAD^+ molecule is shown in yellow, and compound **6** is colored by atom type. The A, B, and C pockets of the NAD^+ binding site are indicated (black letters). The numbers of hydrogen bonds formed are six and five in LiSIR2RP1 and hSIRT1, respectively. In hSIRT1, compound **6** interacts with Arg 274, Ser 442, and Asn 465 in the A pocket and Gln 345 in the B pocket, and is directed away from the C pocket. In LiSIR2RP1 **6** interacts with the adenine sub-pocket (A pocket) and the NAD^+ hydrolysis region (C pocket). The residues involved in hydrogen bonding with compound **6** in LiSIR2RP1 include Ala 40, Gly 216, and Asn 241 present in the A pocket, and Asn 125 in the C pocket. The interaction with the residues of the C pocket may interfere with NAD^+ hydrolysis, and thereby explains its action as an inhibitor.

NAD^+ hydrolysis, and therefore explains its action as an inhibitor. Furthermore, based on a detailed computational analysis, subtle differences in the catalytic and ligand binding domains between LmSIR2 and hSIR2 were recently reported, opening the possibility of selectively targeting the parasite enzyme.^[36] However, co-crystal structure data are needed to establish the binding mode beyond doubt.

Conclusions

For the first time, BNIP derivatives have been identified as a new class of NAD^+ -competitive SIR2 inhibitors that preferentially inhibit the *L. infantum* form of sirtuin (LiSIR2RP1). Furthermore, this study shows that despite the well-conserved catalytic core domain of SIR2 enzymes, subtle structural differences in the inhibitors can provide selective targeting. However, concerns about enzyme selectivity and inhibitory potency, which might be influenced by cellular NAD^+ concentrations, remain the key factors in the development of NAD^+ -competitive SIR2 inhibitors.

Experimental Section

Chemistry

All reagents for syntheses were obtained from Sigma–Aldrich and Fluka, and were used without purification. Thin-layer chromatography (TLC) was performed on Kieselgel 60 F_{254} plates (Merck) in $\text{CHCl}_3/\text{CH}_3\text{OH}$ (97:3 or 99:1). FAB MS data were obtained on a VG Analytical AutoSpec instrument (25 Kv), and low-resolution EC/CI mass spectra were collected on a Micromass Quattro II. For accurate mass, ESI spectra were obtained on Finnigan MAT 900 XLT or 95T spectrometers. ^1H and ^{13}C NMR spectra were recorded on JEOL JNM-EX90 FT and Bruker 400 MHz instruments.

All compounds used in this work, with the exception of (bisnaphthalimidopropylidiamino)pentane (BNIPDapen), -hexane (BNIPDa-hex), -heptane (BNIPDahep), and -dodecane (BNIPDadodec), have been described previously.^[25,26] The synthesis of these compounds is described below.

Step 1: Corresponding diaminopentane, -hexane, -heptane and -dodecane were dissolved in anhydrous pyridine, followed by the addition of mesityl chloride (MesCl; 2.1-fold molar excess). The resulting solution was stirred at room temperature for 4 h. Removal

of the pyridine followed by addition of cold H₂O resulted in the formation of a precipitate. The latter was filtered off and washed thoroughly with H₂O. The crude product was recrystallized from absolute EtOH.

Step 2: Mesitylated diamines (0.651 mmol) were dissolved in anhydrous *N,N*-dimethylformamide (DMF; 13.5 mL) followed by the addition of *O*-tosylpropylnaphthalimide^[26] (0.13 mmol) and Cs₂CO₃ (1.06 g). The solution was left overnight at 80 °C. Completion of the reaction was monitored by TLC. DMF was removed in vacuo, and the residue was poured into cold H₂O. The resulting precipitate was filtered and washed thoroughly with H₂O. After drying, the crude product was recrystallized from EtOH to give the fully protected pure product in high yield (75–85 %).

Step 3: The fully protected polyamine derivatives (0.222 mmol) were dissolved in anhydrous CH₂Cl₂ (10 mL), followed by the addition of hydrobromic acid/glacial acetic acid (1 mL). The solution was left to stir at room temperature for 24 h. The yellow precipitate formed was filtered off and washed with CH₂Cl₂, EtOAc and Et₂O.

BNIPDapen (83 %), ¹H NMR ([D₆]DMSO): δ = 8.48–7.88 (arom), 4.11 (2×N-CH₂), 3.01 (2×N-CH₂), 2.87 (N-CH₂), 2.02 (2×CH₂), 1.60 (2×CH₂), 1.34 ppm (-CH₂-); ¹³C NMR ([D₆]DMSO): δ = 22.91 (2×CH₂), 24.46 (CH₂), 24.79 (CH₂), 36.70 (CH₂), 44.72 (N-CH₂), 46.27 (N-CH₂), 121.99, 127.13, 130.62, 131.21, 134.31 (arom), 163.61 ppm (C=O); HRMS (FAB) calcd for C₃₅H₃₈N₄O₄Br₂: 577.2809 [M-2HBr+H]⁺, found: 577.2827 [M-2HBr+H]⁺.

BNIPDahex (91 %), ¹H NMR ([D₆]DMSO): δ = 8.48–7.88 (arom), 4.09 (2×N-CH₂), 2.99 (2×N-CH₂), 2.86 (N-CH₂), 2.02 (2×CH₂), 1.56 (2×CH₂), 1.27 ppm (2×-CH₂-); ¹³C NMR ([D₆]DMSO): δ = 24.52 (CH₂), 25.21 (CH₂), 25.39 (CH₂), 36.72 (CH₂), 44.81 (N-CH₂), 46.54 (N-CH₂), 121.99, 127.13, 130.62, 131.21, 134.31 (arom), 163.61 ppm (C=O); HRMS (FAB) calcd for C₃₆H₄₀N₄O₄Br₂: 752.510, 671.2227 [M-Br]⁺, found: 671.2221 [M-Br]⁺.

BNIPDahep (94 %), ¹H NMR ([D₆]DMSO): δ = 8.48–7.87 (arom), 4.11 (2×N-CH₂), 2.99 (2×N-CH₂), 2.86 (N-CH₂), 2.02 (2×CH₂), 1.54 (2×CH₂), 1.25 ppm (3×-CH₂-); ¹³C NMR ([D₆]DMSO): δ = 24.46 (CH₂), 25.30 (CH₂), 25.66 (CH₂), 27.84 (CH₂), 36.70 (CH₂), 44.72 (N-CH₂), 46.60 (N-CH₂), 121.99, 127.13, 130.62, 131.21, 134.31 (arom), 163.58 ppm (C=O); HRMS (FAB) calcd for C₃₇H₄₂N₄O₄Br₂: 760.74, 605.3122 [M-2HBr+H]⁺, found: 605.3126 [M-2HBr+H]⁺.

BNIPDadodec (80 %), ¹H NMR ([D₆]DMSO): δ = 8.47–7.87 (arom), 4.11 (2×N-CH₂), 3.00 (2×N-CH₂), 2.85 (N-CH₂), 2.04 (2×CH₂), 1.55 (2×CH₂), 1.22 ppm (4×-CH₂-); ¹³C NMR ([D₆]DMSO): δ = 24.46 (CH₂), 25.39 (CH₂), 25.84 (CH₂), 28.40 (CH₂), 28.73 (CH₂), 28.82 (CH₂), 36.70 (CH₂), 44.72 (N-CH₂), 46.60 (N-CH₂), 121.99, 127.13, 130.62, 131.21, 134.31 (arom), 163.64 ppm (C=O); HRMS (FAB): calcd for C₄₂H₅₂N₄O₄Br₂: 836.709, 755.3166 [M-Br]⁺, found: 755.3168 [M-Br]⁺.

Compounds: Sirtinol, nicotinamide, and suramin were purchased from Sigma. Stock solutions of nicotinamide and suramin were prepared in phosphate-buffered saline (PBS), and the other compounds in DMSO, and they were all stored at -20 °C. Working solutions were freshly diluted in the enzyme reaction buffer to reach the desired final concentrations.

Biological assays

Fluorimetric deacetylase assay of rLiSIR2RP1 and hSIRT1: LiSIR2RP1 (N-terminal His₆ tag) was expressed in *E. coli* and purified by affinity chromatography, as previously reported by our research

group.^[23] The effects of the compounds on NAD⁺-dependent deacetylase activity of the parasite (LiSIR2RP1) and human (SIRT1) forms of the enzyme were assessed by using a commercially available CycLex SIRT1/Sir2 deacetylase fluorimetric kit (CycLex Co. Ltd., Nagano, Japan). This assay system allows the detection of a fluorescent signal upon deacetylation of the peptide substrate, followed by cleavage through the action of a protease. Fluorescence was measured in a fluorimetric microplate reader (Synergy HT, BIO-TEK) with excitation and emission wavelengths set at 340 and 440 nm, respectively. Reactions were performed in the presence of 200 μM NAD⁺, 10 μM acetylated peptide, and each of the inhibitors at a range of various concentrations.

The inhibitory effect of the drugs on rLiSIR2RP1 and hSIRT1 activity is expressed as a percentage, and was calculated according to the ratio between the rates of the enzymatic reaction in the first 20 min in the presence and absence of the inhibitor.

Growth inhibition assays: The growth of LUC-expressing amastigotes in the human leukemia monocyte cell line (THP-1 cells) was evaluated according to Sereno et al.^[38] with some modifications. Briefly, THP-1 cells were cultured in RPMI 1640 medium (Cambrex) supplemented with 10 % heat-inactivated fetal bovine serum (FBS; Cambrex), 2 mM L-glutamine (Cambrex), 100 U mL⁻¹ penicillin (Cambrex), and 100 μg mL⁻¹ streptomycin (Cambrex). Log-phase THP-1 cells were differentiated by incubation for 2 days in medium containing 20 ng mL⁻¹ PMA (Sigma). Once differentiated, the cells became adherent and were washed with pre-warmed medium and then infected with stationary axenic amastigotes expressing LUC at a parasite/macrophage ratio of 3:1 for 4 h at 37 °C under an atmosphere containing 5 % CO₂. Non-internalized parasites were removed, and serial dilutions of each drug were added. After 3 days of incubation at 37 °C under 5 % CO₂, the cells were washed and the luciferase activity was determined.

The luciferase activity of the LUC-expressing parasites was determined as described elsewhere,^[39] and the values were expressed as relative light units (RLU). The percentage of growth inhibition was calculated as (1-RLU of drug-treated parasites)/(RLU drug-untreated parasites)×100. The IC₅₀ values (concentration required to inhibit growth by 50%) were determined by linear regression analysis.

All compounds were initially tested in uninfected THP-1 cells before being incubated with macrophages harboring intracellular amastigotes, and the cytotoxicity was evaluated by MTT assay. Indeed, drug concentrations that were toxic toward uninfected macrophages were not used in the assays to determine IC₅₀ values against intracellular amastigotes (data not shown).

Tubulin deacetylation assay: The deacetylation reactions in which tubulin was used as a substrate were performed with purified tubulin (Pure, Cytoskeleton Inc). The reactions were carried out in deacetylase buffer (10 mM Tris-HCl pH 8.0, 10 mM NaCl) containing 0.5 μg of either tubulin and LiSIR2RP1, in the presence or absence of 1 mM NAD⁺, and left overnight with constant agitation at room temperature. The inhibitors, **7** and nicotinamide, were tested at concentrations of 0, 0.125, 0.250, and 0.5 mM. The amount of DMSO present in the tested concentrations for compound **7** was included as a control. The reactions were stopped by adding 5× Laemmli sample buffer; the proteins were separated by 10 % SDS-PAGE and then subjected to western blot. The nitrocellulose membrane was probed with the following antibodies: mouse monoclonal anti-(acetylated tubulin) antibody (clone 6-11B-1) from Sigma; mouse monoclonal anti-(α-tubulin) antibody (clone DM1A) from

NeoMarkers, and the mouse monoclonal antibody IIIG4, produced as described by Vergnes and colleagues.^[21]

Computational methods

Modeling and docking of inhibitors: Homology modeling was done for hSIRT1 and LiSIR2RP1 by using the comparative protein modeling program MODELLER. The crystal structure of human SIRT2 (PDB code: 1J8F) was used as a template in both cases. Sequences were aligned with the align2d command in MODELLER. The optimization of the models was done using molecular dynamics (MD) with the simulated annealing (SA) method in MODELLER. Out of the five models generated for each protein, the best model was evaluated based on the lowest MODELLER Objective function. The quality and geometry of models was checked using the program PROCHECK and VERIFY_3D in SAVES server. The NAD⁺ molecule was added to the models using MOE. These models were then subjected to further refinement and energy minimization using the Biopolymer module in Sybyl. Molecular surface was generated using the Molcad module in Sybyl to analyze and compare the binding pocket of NAD⁺ in both structures. Four BNIP derivatives—**3**, **6**, **7**, and **8**—showing a range of IC₅₀ values, were selected to perform docking for LiSIR2RP1 and hSIRT1 using the FlexX module in Sybyl.

Statistical analysis: The data were analyzed using Student's *t* test.

Acknowledgements

This work was funded by the Fundação para a Ciência e Tecnologia (FCT) POCI 2010 and co-funded by FEDER grant number POCI/SAU-FCF/59837/2004, Centre Franco Indien pour la promotion de la recherche avancée; Indo–French Centre for the promotion of advanced research (CEFIPRA/IFCPAR) grant number 3603, and INSERM. Thanks to the EPSRC National Mass Spectrometry Service Centre at Swansea University, Swansea (UK) for mass spectral analysis, and the Treaty of Windsor Anglo–Portuguese Joint Research Programme for funding. J.T. is supported by a fellowship from FCT number SFRH/BD/18137/2004. The authors thank A. Ferreira for the English revision of the manuscript.

Keywords: docking • NAD⁺-dependent deacetylases • protozoa • sirtuin inhibitors

- [1] C. B. Brachmann, J. M. Sherman, S. E. Devine, E. E. Cameron, L. Pillus, J. D. Boeke, *Genes Dev.* **1995**, *9*, 2888–2902.
- [2] K. Zhao, R. Marmorstein, in *Histone Deacetylases: Transcriptional Regulation and Other Cellular Functions* (Ed.: E. Verdin), Humana, Totowa NJ, **2006**, 203–217.
- [3] S. Imai, C. M. Armstrong, M. Kaerberlein, L. Guarente, *Nature* **2000**, *403*, 795–800.
- [4] B. J. North, B. L. Marshall, M. T. Borra, J. M. Denu, E. Verdin, *Mol. Cell* **2003**, *11*, 437–444.
- [5] V. J. Starai, I. Celic, R. N. Cole, J. D. Boeke, J. C. Escalante-Semerena, *Science* **2002**, *298*, 2390–2392.
- [6] A. A. Sauve, V. L. Schramm, *Curr. Med. Chem.* **2004**, *11*, 807–826.
- [7] G. Liszt, E. Ford, M. Kurtev, L. Guarente, *J. Biol. Chem.* **2005**, *280*, 21313–21320.
- [8] S. Pagans, A. Pedal, B. J. North, K. Kaehlcke, B. L. Marshall, A. Dorr, C. Hetzer-Egger, P. Henklein, R. Frye, M. W. McBurney, H. Hruby, M. Jung, E. Verdin, M. Ott, *PLoS Biol.* **2005**, *3*, e41.

- [9] H. Vaziri, S. K. Dessain, E. Ng Eaton, S. I. Imai, R. A. Frye, T. K. Pandita, L. Guarente, R. A. Weinberg, *Cell* **2001**, *107*, 149–159.
- [10] O. R. Bereshchenko, W. Gu, R. Dalla-Favera, *Nat. Genet.* **2002**, *32*, 606–613.
- [11] H. Ota, E. Tokunaga, K. Chang, M. Hikasa, K. Iijima, M. Eto, K. Kozaki, M. Akishita, Y. Ouchi, M. Kaneki, *Oncogene* **2006**, *25*, 176–185.
- [12] T. F. Outeiro, E. Kontopoulos, S. M. Altmann, I. Kufareva, K. E. Strathearn, A. M. Amore, C. B. Volk, M. M. Maxwell, J. C. Rochet, P. J. McLean, A. B. Young, R. Abagyan, M. B. Feany, B. T. Hyman, A. Kazantsev, *Science* **2007**, *317*, 516–519.
- [13] C. M. Grozinger, E. D. Chao, H. E. Blackwell, D. Moazed, S. L. Schreiber, *J. Biol. Chem.* **2001**, *276*, 38837–38843.
- [14] A. Bedalov, T. Gattabont, W. P. Irvine, D. E. Gottschling, J. A. Simon, *Proc. Natl. Acad. Sci. USA* **2001**, *98*, 15113–15118.
- [15] A. Mai, S. Massa, S. Lavu, R. Pezzi, S. Simeoni, R. Ragno, F. R. Mariotti, F. Chiani, G. Camilloni, D. A. Sinclair, *J. Med. Chem.* **2005**, *48*, 7789–7795.
- [16] R. C. Neugebauer, U. Uchieschowska, R. Meier, H. Hruby, V. Valkov, E. Verdin, W. Sippl, M. Jung, *J. Med. Chem.* **2008**, *51*, 1203–1213.
- [17] A. D. Napper, J. Hixon, T. McDonagh, K. Keavey, J. F. Pons, J. Barker, W. T. Yau, P. Amouzegh, A. Flegg, E. Hamelin, R. J. Thomas, M. Kates, S. Jones, M. A. Navia, J. O. Saunders, P. S. DiStefano, R. Curtis, *J. Med. Chem.* **2005**, *48*, 8045–8054.
- [18] K. T. Howitz, K. J. Bitterman, H. Y. Cohen, D. W. Lamming, S. Lavu, J. G. Wood, R. E. Zipkin, P. Chung, A. Kisielewski, L. L. Zhang, B. Scherer, D. A. Sinclair, *Nature* **2003**, *425*, 191–196.
- [19] J. Trapp, R. Meier, D. Hongwiset, M. U. Kassack, W. Sippl, M. Jung, *ChemMedChem* **2007**, *2*, 1419–1431.
- [20] A. Schuetz, J. Min, T. Antoshenko, C. L. Wang, *Structure* **2007**, *15*, 377–389.
- [21] B. Vergnes, D. Sereno, N. Madjidian-Sereno, J. L. Lemesre, A. Ouaisi, *Gene* **2002**, *296*, 139–150.
- [22] B. Vergnes, D. Sereno, J. Tavares, A. Cordeiro-da-Silva, L. Vanhille, N. Madjidian-Sereno, D. Depoix, A. Monte-Alegre, A. Ouaisi, *Gene* **2005**, *363*, 85–96.
- [23] J. Tavares, A. Ouaisi, N. Santarém, D. Sereno, B. Vergnes, P. Sampaio, A. Cordeiro-da-Silva, *Biochem. J.* **2008**, *415*, 377–386.
- [24] J. Tavares, A. Ouaisi, P. K. T. Lin, A. Tomás, A. Cordeiro-da-Silva, *Int. J. Parasitol.* **2005**, *35*, 637–646.
- [25] P. K. T. Lin, V. A. Pavlov, *Bioorg. Med. Chem. Lett.* **2000**, *10*, 1609–1612.
- [26] J. Oliveira, L. Ralton, J. Tavares, A. Codeiro-da-Silva, C. S. Bestwick, A. McPherson, P. K. Thoo Lin, *Bioorg. Med. Chem.* **2007**, *15*, 541–545.
- [27] A. M. Dance, L. Ralton, Z. Fuller, L. Milne, S. Duthie, C. S. Bestwick, P. K. T. Lin, *Biochem. Pharmacol.* **2005**, *69*, 19–27.
- [28] A. A. Sauve, I. Celic, J. Avalos, H. Deng, J. D. Boeke, V. L. Schramm, *Biochemistry* **2001**, *40*, 15456–15463.
- [29] J. M. Denu, *Trends Biochem. Sci.* **2003**, *28*, 41–48.
- [30] M. D. Jackson, M. T. Schmidt, N. J. Oppenheimer, J. M. Denu, *J. Biol. Chem.* **2003**, *278*, 50985–50998.
- [31] J. L. Avalos, K. M. Bever, C. Wolberger, *Mol. Cell* **2005**, *17*, 855–868.
- [32] J. C. Tanny, D. S. Kirkpatrick, S. A. Gerber, S. P. Gygi, D. Moazed, *Mol. Cell Biol.* **2004**, *24*, 6931–6946.
- [33] T. E. Voogd, E. L. Vansterkenburg, J. Wilting, L. H. Janssen, *Pharmacol. Rev.* **1993**, *45*, 177–203.
- [34] A. Monte-Alegre, A. Ouaisi, D. Sereno, *Kinetoplastid Biol. Dis.* **2006**, *23*, 5–6.
- [35] J. Trapp, A. Jochum, R. Meier, L. Saunders, B. Marshall, C. Kunick, E. Verdin, P. Goekjian, W. Sippl, M. Jung, *J. Med. Chem.* **2006**, *49*, 7307–7316.
- [36] R. U. Kadam, V. M. Kiran, N. Roy, *Bioorg. Med. Chem. Lett.* **2006**, *16*, 6013–6018.
- [37] M. S. Finnin, J. R. Donigan, N. P. Pavletich, *Nat. Struct. Biol.* **2001**, *8*, 621–625.
- [38] D. Sereno, G. Roy, J. L. Lemesre, B. Papadopoulou, M. Ouellette, *Antimicrob. Agents Chemother.* **2001**, *45*, 1168–1173.
- [39] G. Roy, C. Dumas, D. Sereno, Y. Wu, A. K. Singh, M. J. Tremblay, M. Ouellette, M. Olivier, B. Papadopoulou, *Mol. Biochem. Parasitol.* **2000**, *110*, 195–206.

Received: September 3, 2009

Revised: October 29, 2009

Published online on November 20, 2009